

Photoluminescence of MEH-PPV Brushes, Pancakes, and Free Molecules in Solutions and Dry States

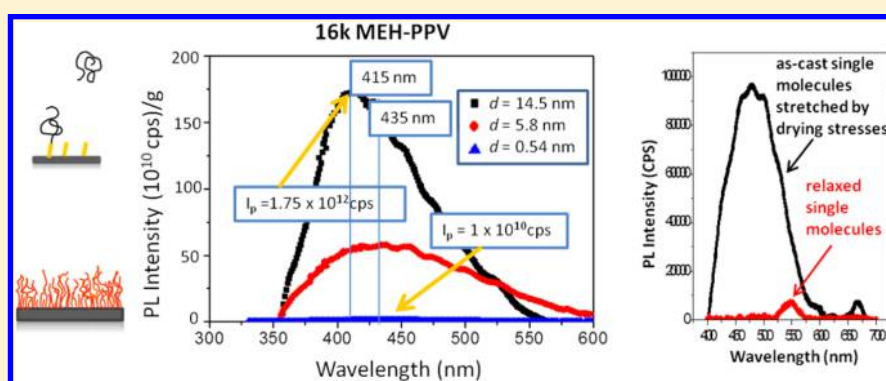
Kuo Sheng Shih,^{†,‡} Chien Chung Chen,^{‡,§} Po-Tsun Chen,[†] Ya-Wei Yang,[†] Jonathon D. White,^{||} Yu-Ming Chang,[⊥] and Arnold Chang-Mou Yang^{*,†,§}

[†]Department of Materials Science and Engineering and [§]Instrumentation Center, National Tsing Hua University, Hsinchu 300, Taiwan

^{||}Department of Optoelectronics, Yuan Ze University, Taoyuan 320, Taiwan

[⊥]Center of Condensed Matter Sciences, National Taiwan University, Taipei 100, Taiwan

S Supporting Information



ABSTRACT: Photoluminescence (PL) of a conjugated polymer MEH-PPV, poly[2-methoxy-5-(2'-ethylhexyl)oxy]-1,4-phenylenevinylene], grafted on a silicon wafer with controlled tether spacing was studied to reveal the effects of molecular conformation, chain packing, and mechanical stress. In the solvent-swollen state, the PL of the densely grafted polymer (denoted “brushes”) was blue-shifted substantially relative to the lightly grafted (denoted “pancakes”) and free polymers. As solvent evaporated, while for the brushes the changes in PL were insignificant, the PL spectra of the pancakes underwent large blue shifts and exhibited significant efficiency enhancements up to ~175-fold. The solvent evaporation effects were attributed to molecular deformations resulting from coil contraction on the substrate, which gave rise to conjugation-disruptive kinks (blue shift) and segmental stretching (PL enhancement) in the dried molecules. Moreover, heterojunctional quenching was found significantly suppressed by the mechanical stresses. Similar behavior was observed in dried free single molecules. These results unveil the fundamental role of mechanical stresses, not only indirectly through their influence on molecular conformations, but directly via alterations of the excitonic behavior.

KEYWORDS: organic electronics, conjugated polymers, optoelectronic efficiencies, mechanical stresses, molecular conformation, solar cells, light emitting diodes, photonics

Poor quantum efficiencies still hurdle the prevalence of the otherwise very promising conjugated polymers (CPs) for ubiquitous optoelectronic applications, such as light-emitting diodes, solar panels, and phosphors. Despite many years of study, our understanding of the physics associated with optical or electrical excitation in solid CP films and the subsequent energy transfer remain highly limited.^{1–4} The efficiency of the solid films composed of CP molecules is generally thought to be hindered by “excited state trapping”, a characteristic normally taken as intrinsic to the amorphous solids.^{10–15} Nevertheless, the long continuous π -orbital conjugation along the molecular backbones has long been deemed as advantageous for macroscopic energy transfer over what are offered by the small-molecule counterparts.

Recently, strong evidence has revealed that molecular conformation (and morphology) appears to be pivotal in the energy transfer in CPs.^{5–10,14,15} The large discrepancies in quantum efficiency among the solid films and solutions of similar molecular conformations, however, have prompted questions for theories based exclusively on molecular conformations. Subsequently, dramatic increases of photoluminescence (PL) efficiencies were reported when CP molecules were mechanically stretched.^{16–18} The enhancements were attributed to suppression of electron–phonon interactions in the stress-rigidified molecular strands,¹¹ which is,

Received: September 11, 2013

Published: December 3, 2014

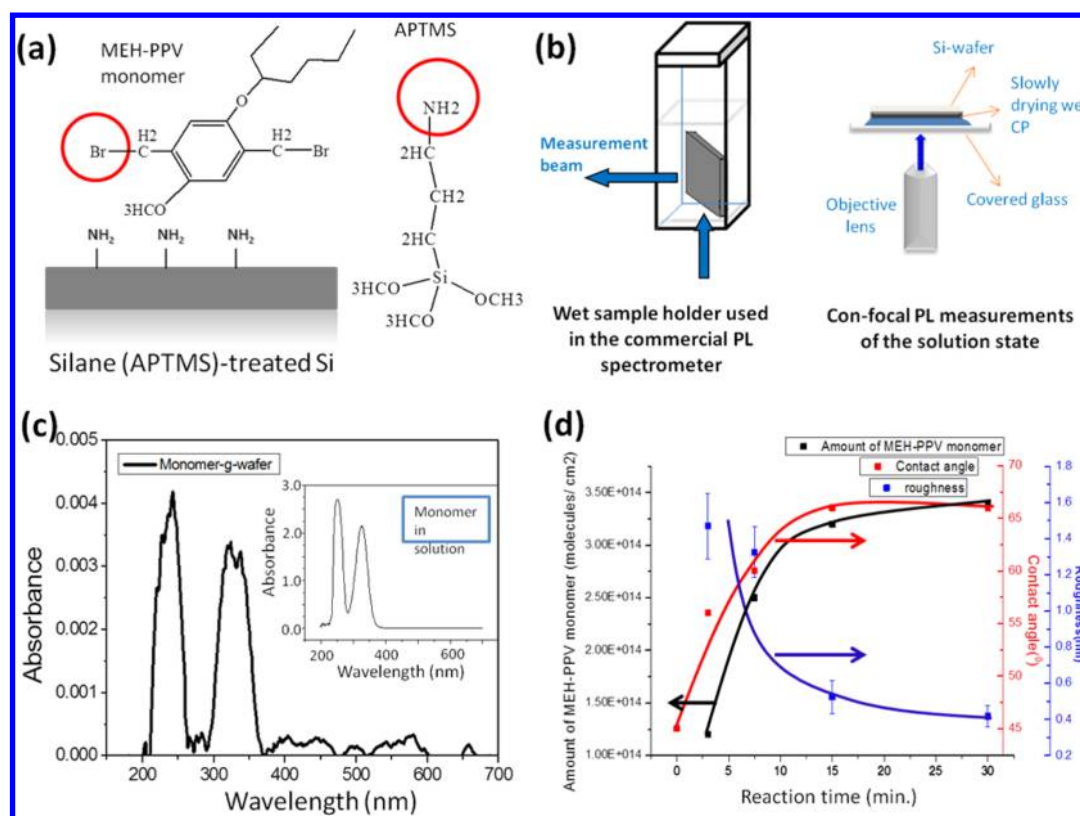


Figure 1. (a) Schematic depiction of the molecular structures of MEH-PPV monomer, APTMS primer, and the primed silicon surface. (b) Schematic depiction of the sample holders of the wet specimens used in the commercial PL spectrometer (left) and confocal micro-PL system (right). (c) UV–visible spectrum of the APTMS-primed Si-wafer grafted with a monolayer of MEH-PPV monomer. (d) Variations of the graft mass (of MEH-PPV monomer), contact angle, and surface roughness during the growth of the monomer monolayer as a function of reaction time.

in fact, consistent with the efficiency enhancements observed in the rigidified CPs via tailored synthesis.^{19–21} Furthermore, it was found that for sufficiently large mechanical forces, heterojunction quenching at interfaces may be effectively switched-off,^{17,18} implying the fundamental role of electron–phonon coupling in the formation and behavior of the excitons.

Since the mechanical stress applied to a molecular segment imposes new equilibrium conditions, via restricting the rotation of individual bonds, for the end-to-end distance, it is intimately connected to the chain conformation for polymers in general. Nevertheless, molecular stress and molecular conformation are different subjects carrying distinctive physical meanings and hence discernment is required. For example, mechanical relaxation occurring in solid polymers may lead to substantial reduction in mechanical stress but not necessarily large alterations for the ensemble-averaged molecular conformation. Obviously, it is important to recognize the interconnections between the two, while keen to differentiate the effects arising from one from those of the other.

In this work, various molecular conformations (brushes, pancakes, and free molecules) of CPs were prepared via designed synthesis and the PL behavior was studied in both the solution and the dry states, where the mechanical stress induced by solvent evaporation, similar to that observed as residual stress in solution-cast ultrathin polymer films,^{17,18,22,23} was exploited to unveil the mechanical stress effects on the CP photonic behavior. It was found that the drying stress had fostered a very pronounced effect on the conformation-specified CPs. The results may shed light on the energy

transfer mechanisms in CPs and provide useful clues for the development of high efficiency applications based on them.

EXPERIMENTAL SECTION

Synthesis of MEH-PPV Monomer and Polymers. MEH-PPV monomer was synthesized (reaction scheme see Figure S1, Supporting Information)²⁴ by first mixing 4-methoxyphenol (6 g), KOH (3.36 g), tetrabutyl-ammonium bromide (0.3 g), and deionized water (22 mL) mechanically at room temperature to form a uniform solution. 2-Ethylhexyl bromide (9 mL) was then added and the stirring continued at 100 °C for 3 days. The top portion of the solution was collected and reacted with paraformaldehyde (1.78 g), HBr (18 mL), and acetic acid (45 mL) at 70 °C for 4 h before crystallizing at 4 °C. The residual HBr was removed and the crystals were dissolved in hexane. After filtration and neutralization with the KOH solution, the light yellow liquid at the top was collected and dried in a fume hood, which yielded the MEH-PPV monomer.

To polymerize, the monomer (625 mg) was dissolved in THF (75 mL) before adding the initiator potassium *tert*-butoxide (*t*-BuOK) solution (*t*-BuOK (468 mg) in THF (40 mL) by sonication). The reaction took place in the dark at 2–4 °C for 4 h. After filtration, the MEH-PPV polymer was precipitated in excess methanol. The molar mass (*M*) of the MEH-PPV was controlled by the amount of the *t*-BuOK solution.^{24,25} Two molar masses were synthesized: *M* = 16 kg/mol (dispersity ~ 1.05) and *M* = 55 kg/mol (dispersity ~ 1.20).²⁶ The chemical structure of the polymer was characterized by using ¹H NMR (500 MHz, CDCl₃) and the tolane-bis-benzyl (TBB) defects^{27,28} were found to be ~0.65 wt

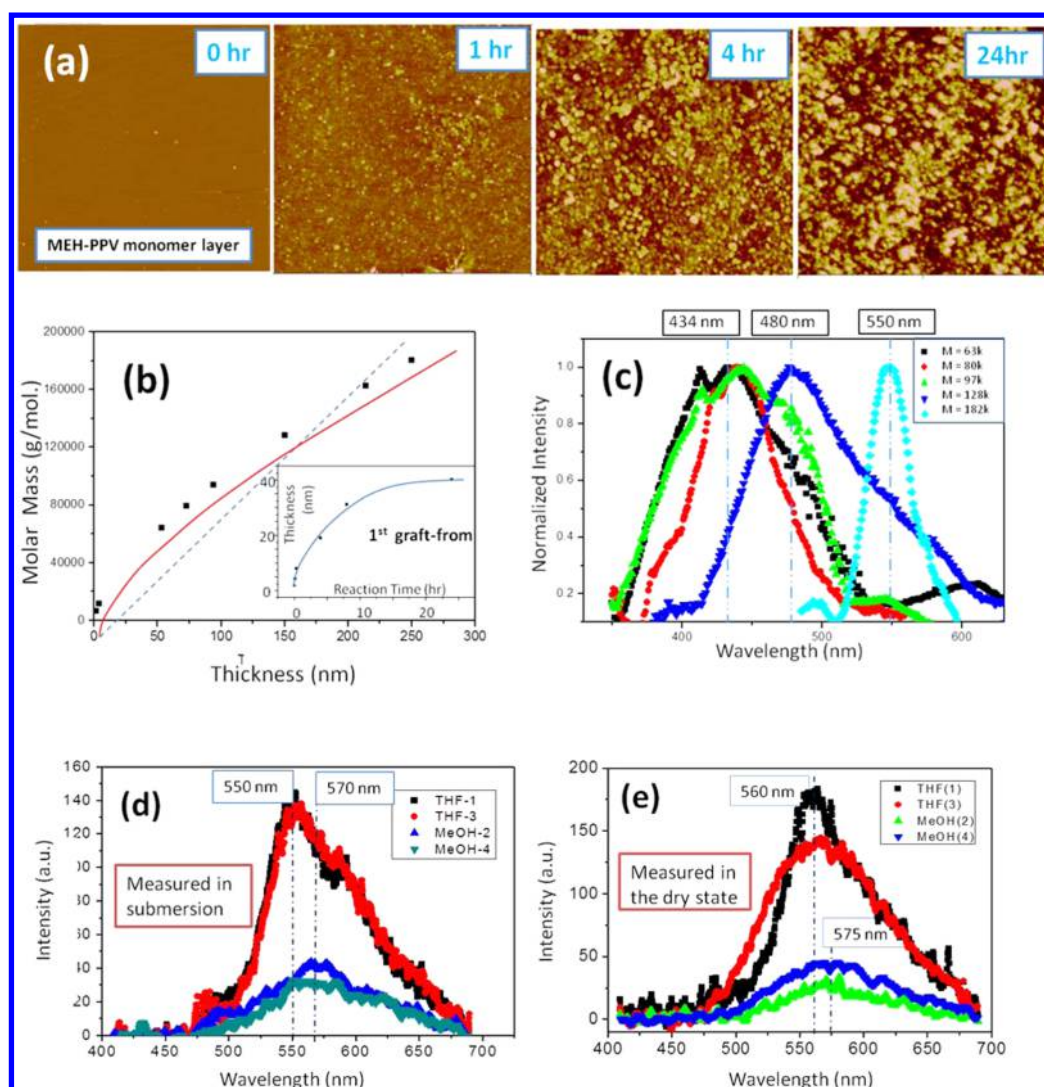


Figure 2. Characteristics of the MEH-PPV brush molecules grown in the “graft-from” reaction. (a) SFM topography at various reaction times in the first graft-from reaction at 60 °C (scan size: 20 $\mu\text{m} \times 20 \mu\text{m}$). (b) Molar mass of the brushes vs total thickness, (inset) layer thickness as a function of reaction time during the first graft-from reaction. (c) PL spectra of the dry MEH-PPV brushes for various Ms. (d) PL spectra of the MEH-PPV brush sample ($M = 182 \text{ kg/mol}$) acquired while it was submerged, respectively, in THF, MeOH, and again THF, and MeOH. (e) PL spectra of the MEH-PPV brush sample ($M = 182 \text{ kg/mol}$) measured in air after it was submerged, respectively, in THF, MeOH, then again THF, and MeOH.

% for the $M = 55 \text{ kg/mol}$ and not detectable for the $M = 16 \text{ kg/mol}$, suggesting that the average distance between defects for the free polymer was ~ 154 monomers.

Substrate Priming. Priming of the Si-wafer substrate, required for polymer grafting, comprised of a series of steps, namely, (a) growing a complete monolayer of Si-OH on the wafer,^{29–32} followed by (b) adsorption of self-assembling 3-aminopropyltrimethoxysilane (APTMS) molecules (Figure 1a),^{33–43} (c) curing to convert the OH-Si physisorption into Si-O-Si bonding via APTMS flipping,^{34,36,43} and finally (d) reacting the cured APTMS-Si wafer with MEH-PPV monomer (at the absence of the *t*-BuOK initiator) to clad a monomer monolayer on the wafer surface. The anchored monomer served as a seeding site for growing a MEH-PPV chain in the subsequent polymerization reaction (“graft-from” reaction) or chemically bonding a presynthesized MEH-PPV macromolecule (“graft-to”; Figure 1a). The existence of the complete monomer layer was confirmed by measurements of contact angles, UV-visible spectra (Figure 1c), and roughness of the grafted surface (Figure 1d). Further details of the

priming processes are given in the Supporting Information, section 2.

MEH-PPV Grafting. For the “graft-from” reactions,^{24,33,44–46} the primed substrate was immersed in the *t*-BuOK solution (188 mg in 16 mL THF) with the monomer (250 mg in 30 mL THF) slowly dripped in. The thickness of the grafted layer was measured by using a scanning force microscope (SFM) on the scratched dried samples. Growth eventually slowed due to monomer exhaustion (inset, Figure 2b). Hence, for growing longer brushes, graft polymerization was carried out in two steps: first at a temperature of 60 or 70 °C for 12 h (Figure 2a),²⁴ and then at 78 °C in the presence of a higher *t*-BuOK concentration. When the polymerization was completed, the wafer was sonicated in DI water to remove residual *t*-BuOK, followed by sonication in THF (30 min) to remove the adsorbed free MEH-PPV polymer.

For the “graft-to” reactions,^{26,47,48} the primed substrate was reacting with the prepolymerized MEH-PPV dissolved in equal-part THF, toluene, and cyclohexanone ($\sim 24 \text{ h}$, filtered via 0.45 μm pores) at 70 °C. The graft density was controlled by the

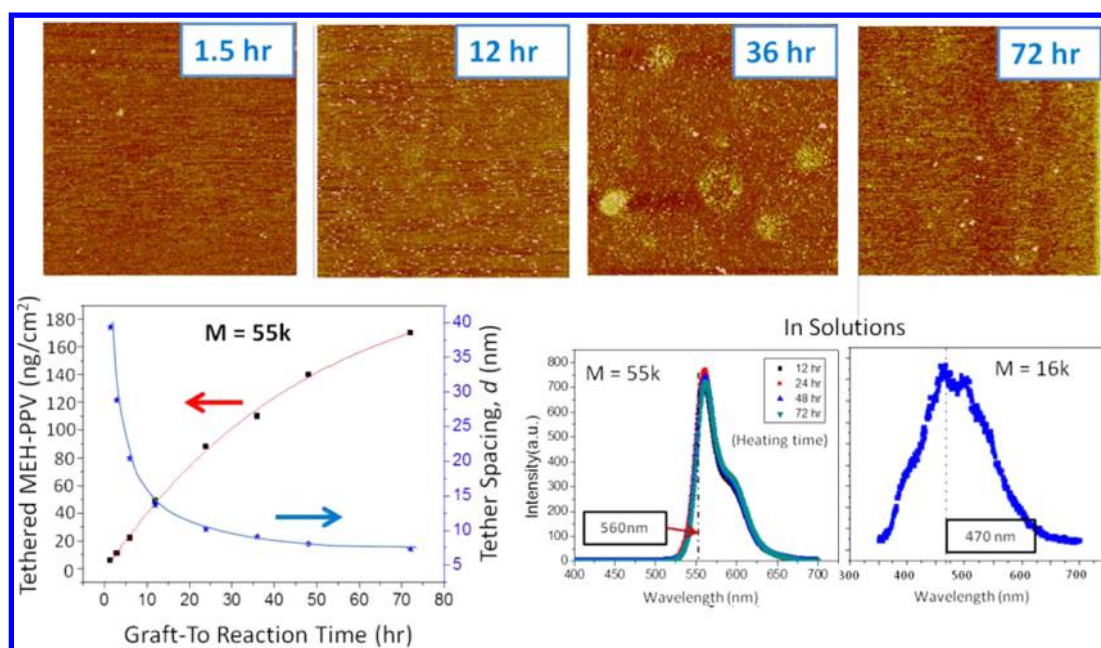


Figure 3. Characteristics of the MEH-PPV pancake molecules ($M = 55$ kg/mol) attached in the “graft-to” reaction. (top) Evolution of the graft surface topography during the graft-to reaction ($c = 2.5$ mg/cm³, in air; scan size: $20\ \mu\text{m} \times 20\ \mu\text{m}$, maximum topographic height: 3 nm). (bottom left) Grafted amount and the tether spacing as a function of reaction time; (bottom right) PL spectra of the free MEH-PPV polymers ($M = 16$ and 55 kg/mol) in solution, showing that MEH-PPV was stable during the reaction at 70 °C.

reaction time (up to 72 h). The heating used for the reactions was proved to not cause any degradation of the polymers, as verified by the PL spectra (Figure 3). After the grafting reaction, the samples were rinsed in THF under sonication for 30 min to remove the nongrafted polymers. Two polymer concentrations were used, one near c^* (~ 2.5 mg/mL) and the other substantially lower (0.06 mg/mL). The grafting of the MEH-PPV molecules was confirmed by the FT-IR spectra (not shown)⁴⁹ showing the emergence of the out-of-plane phenyl CH wag at $858\ \text{cm}^{-1}$, the alkyl-oxygen stretching at $1040\ \text{cm}^{-1}$, the phenyl oxygen stretching at $1204\ \text{cm}^{-1}$, and the semicircular phenyl stretching at $1506\ \text{cm}^{-1}$ amid the diminishing of the characteristic APTMS peak at $3371\ \text{cm}^{-1}$ due to NH_2 consumption for grafting.

Characterization. The grafted polymer films were analyzed by using the SFMs (Veeco Nanoscope V and Dimension 3100), a UV–visible spectrometer (Hitachi U3010), photoluminescence (PL) spectrometers (Horiba Jobin Yvon Fluorolog-3 and PerkinElmer LS55), an FT-IR (Horiba F730), and a home-built confocal micro-PL spectrometer integrated with a SFM (Catalyst II, Bruker). For measurements using the PerkinElmer spectrometer, the excitation (collection) was at an angle of 45° (60°) relative to the sample. For the Horiba PL spectrometer both excitation and detection were at 45° relative to the film plane (Figure 1b). In the commercial PL spectrometers (the Horiba and PerkinElmer), different sample holders were required and used for the dry and solvent-submerged samples, but it was still possible to compare the PL intensities of the dry and solvent-swollen samples obtained from the PL spectrometers (the Horiba and PerkinElmer) after proper calibration was taken. The SFM-integrated confocal micro-PL spectrometer was used to probe local regions in the samples for the PL properties. In this case, the excitation beam was incident normal to the sample, while the emissions were collected along the same path but reversed at 180° . The confocal setup also consisted of an inverted optical microscope

(Olympus IX71), laser sources (473 and 632.8 nm), and optical detector (Princeton Instrument, SP2300).

In all our experiments, the effect of light absorption by solvent molecules during the PL measurements was neglected as the excitation wavelengths were substantially higher than the solvent absorption thresholds (typically below 300 nm).

The “graft-from” reactions produced tightly packed “MEH-PPV brushes”⁴⁴ because the average tether distance (d ; ~ 0.54 nm) was smaller than the full length of the MEH-PPV monomer sidegroup (~ 0.9 nm) and substantially below the radius of gyration (R_g) of the attached MEH-PPV molecules. In contrast, the “graft-to” reactions yielded lightly tethered polymer molecules spaced far apart on the substrate (~ 6 to ~ 40 nm, as controlled by reaction time and molecular size), and hence, these tethered polymer molecules were regarded as MEH-PPV pancakes. It may be constructive to point out that generally it is challenging to probe the monolayer graft in either the solvent-swollen or dry state due to the tiny sample sizes and the likelihood of probe-inflicted sample alterations. However, the molecular conformation and chain packing of the grafted MEH-PPV can be reliably assumed on the grounds of careful synthesis and rigorous sample preparation and checked by detailed characterization, as to be presented in the following.

RESULTS AND DISCUSSIONS

Primer Layer. The tether spacing d in the APTMS monolayer (thickness ~ 0.7 nm, by SFM) was determined from measurements of the graft amount of MEH-PPV monomer, S , in the reaction with the cured APTMS-Si wafer without the t -BuOK initiator. The graft amount S , determined from the UV–visible spectra (Figure 1c) via $S = A/\epsilon$, where A is the sample absorption and ϵ is the MEH-PPV monomer absorption coefficient ($\epsilon = 1.76 \times 10^7\ \text{mol}^{-1}\cdot\text{cm}^2$) measured separately (inset, Figure 1b), was found to increase almost linearly with the graft time but saturated at 3.5×10^{14} APTMS molecules/cm² after ~ 15 min, corresponding to $d \sim 0.54$ nm

(Figure 1d). This graft density is in good agreement with the reported maximum silane tether density on a Si-wafer of 5.0×10^{14} molecules/cm².^{36,42}

Brush Molecules. As seen in the SFM images of the dried sample (Figure 2a), the topography was smooth for short reaction times. As the molecules increased in length, small bumps started to emerge and gradually increased in lateral size with time, to $\sim 0.1 - 2 \mu\text{m}$ at 24 h. As discussed by Siqueira et al.,²⁶ these bumps likely resulted from local “bundling” of the longer brush molecules upon drying with the bump size correlated with the molecular length.

Since they grew from the continuous seeding monolayer (see Experimental Section, Substrate Priming), the brush molecules were expected to form a continuous graft layer soon after the very beginning of the graft-from reaction. The graft film was extraordinarily hard and tough, as discovered by mechanical scratching, implicating the tight molecular packing. The molar mass was estimated from the thickness (τ) of the dry graft layer and the graft density ($d = 3.5 \times 10^{14}$ chains/cm²) on the assumption that the occupied volume of each brush molecule could be approximated as that of a free molecule (the Gaussian chain) of the same molecular length based on the fact that the molecules may relax somewhat when dried relatively slowly. For simplicity, a constant overlap concentration c^* (~ 5 wt %) of MEH-PPV was used. The molar mass was estimated to be ~ 63 kg/mol for 3 h at 70 °C ($\tau = 52$ nm) and reach 180 kg/mol after the second-step polymerization (Figure 2b). The estimated M increased approximately linearly as τ increased, with a slope of ~ 800 g·mol⁻¹ nm⁻¹ that was $\sim 2\times$ the ideal value for upright brushes. It indicates that the brush molecules, when in the dry state, were partially relaxed, grouped locally, forming “molecular bundles” and lying down $\sim 60^\circ$ ($\sim \cos^{-1}(1/2)$) from the vertical in random azimuthal directions. Despite being a reasonable assumption, the Gaussian approximation for the molecular volume possibly led to a certain degree of overestimation and, hence, to underestimated molar masses. Were that to be the case, the dry brush molecules would in reality lay down with an angle greater than 60° to the substrate normal. Although the brush molecules deviated substantially from the upright geometry, they were still constrained within the “bundles” by the neighboring molecules tethered on the substrate.

Pancake Molecules. At the beginning of the graft-to reaction, tiny bumps appeared on the SFM topography of the dried samples. Each of these bumps contained, on average, ~ 70 – 100 molecules ($M = 16$ kg/mol) or ~ 200 – 300 molecules ($M = 55$ kg/mol), as estimated from their sizes (Figure 3 (top)). As the reaction proceeded further, the bumps increased in population, gradually connected together, and later covered the whole surface. Eventually, the topography eventually became smooth and uniform, believably due to the removal of the trapped nongrafted molecules when grafting was still occurring at any available sites. The graft amount and tether spacing d were determined from the bearing ratio of the SFM topography (for early stage samples) or layer thickness (for complete layers). For the $M = 55$ kg/mol MEH-PPV, the tether spacing d ranged from 7 nm to ~ 40 nm (Figure 3, bottom left) for which the lower bound ($d \sim 7$ nm) was comparable to the size of the swollen molecules in the solution. Similar behavior was observed for the 16k MEH-PPV, where d ranged from ~ 6 nm to ~ 15 nm (not shown). Generally, the grafting rates were higher for more dilute polymer solutions (e.g., 0.06 mg/mL),

implying the operation of a molecular crowding effect near the substrate during grafting.

Effects of Si-Wafer Substrate on PL. The influences of exciton quenching at the MEH-PPV/Si-wafer heterojunction and PL absorption by the Si-wafer were examined by performing an auxiliary experiment using spin-coated ultrathin (ca. 15–17 nm) MEH-PPV films on various substrates when the PL spectra were taken: (a) Si-wafer, (b) glass slide, (c) Si-wafer coated with a thick polystyrene (PS, ca. 150 nm), and (d) glass slide attached to a reflective metal plate.

It was found that the wavelength of the PL peak (λ_p) was independent of the substrate except a small shift (~ 20 nm) of λ_p to the shorter wavelengths (blue shifting) when the substrate was changed from Si-wafer to glass slide (Figure S4, Supporting Information). The small shift of λ_p is believed due to the slight variation in molecular packing engendered during spin coating of the films by the small difference in the Hamaker constant between the substrates.^{17,18}

In contrast, the PL intensity depended strongly on the substrate. Firstly, on a glass slide that absorbed light negligible in this visible spectral range, the PL intensity of the film doubled approximately when a reflective metal plate was attached to the backside of the substrate (Figure S4, Supporting Information). It indicates the nearly full recovery of the $\sim 50\%$ PL loss through the backside by the reflective plate. Since the bandgap of the glass slide (~ 9.0 eV) is substantially greater than that of the MEH-PPV film (2.34 eV), there was no heterojunction quenching,¹¹ and thus, the PL intensity of the film on glass/metal plate represented the genuine PL behavior unaffected by transmission loss, substrate absorption, and heterojunction quenching.

Secondly, as a Si-wafer was used instead of the glass/metal substrate, the PL intensity plunged $\sim 90\%$ (Figure S4, Supporting Information). The plummet, obviously, was due to quenching at the heterojunction where within the diffusion length (~ 15 – 30 nm) excitons were torn apart by the electric field built by the smaller bandgap of the Si-wafer (1.12 eV) relative to the film.^{11,18} When the optically inert thick PS layer was inserted between the film and the Si-wafer, the quenching was removed substantially. The PL intensity returned to what approximately corresponding to that on the glass/metal plate (Figure S4, Supporting Information). It also indicates that PL absorption by Si-wafer was comparable to that by glass slide and thus negligible.

Therefore, PL absorption by Si-wafer substrate was neglected throughout this work, while heterojunction quenching was always considered carefully, particularly when samples of substantial height differences were compared for the PL intensities.

PL of the Brushes. The PL spectrum of the brushes in the dry state was found constructed by a broad peak that was shifting to longer wavelengths (red-shifting) for increased chain length (e.g., from $\lambda_p \sim 434$ nm for $M = 63$ kg/mol to $\lambda_p \sim 550$ nm for $M = 182$ kg/mol, Figure 2c). When the brushes were transferred from the dry state to submergence in a good solvent (such as THF), a small, negligible red shift (less than ~ 10 nm) was observed (Figures 2d,e). The red shift increased somewhat (~ 15 nm) for poorer solvents (methanol, MeOH). As illustrated, these shifts were reversible upon solvent switch or transferring between the dry and the solvation states. It was thus inferred that, on the length scales concerning the radiative energy propagation, the physical constraints imparted to the brush molecules were effective enough so that only minimal

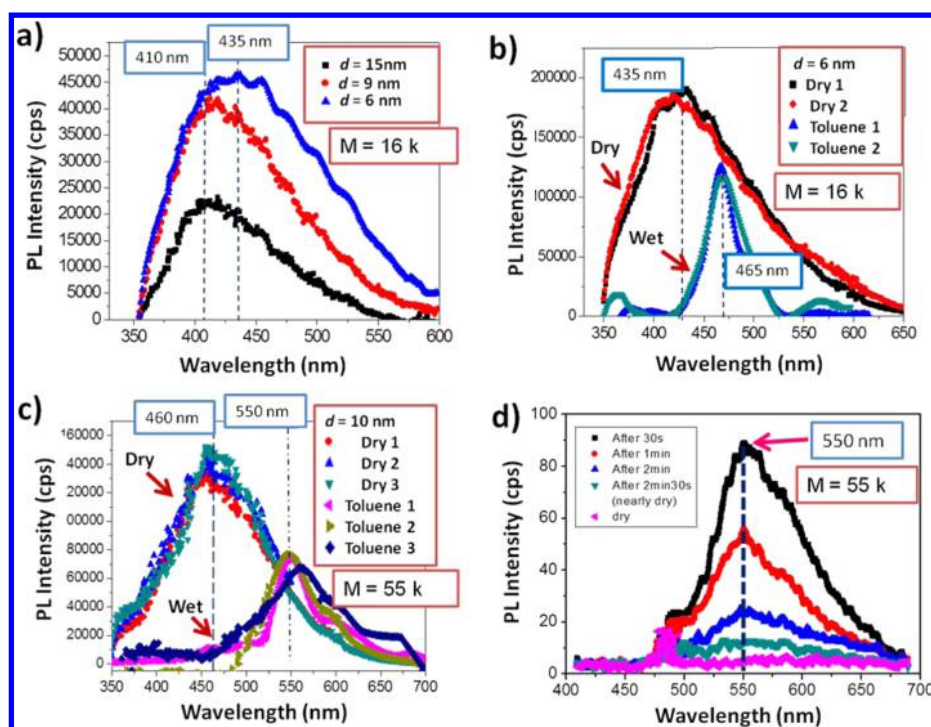


Figure 4. PL spectra of the pancake molecules. (a) PL spectra of the pancakes ($M = 16$ kg/mol) with various tether spacing d s. (b, c) PL spectra of the pancakes transported between the dry and solvent-swollen state for $M = 16$ and 55 kg/mol. (d) The confocal PL spectra as a function of drying time of the slowly dried pancakes ($M = 55$ kg/mol).

conformation alterations were produced upon the drastic change from solvation to dry state. On the other hand, the molecules under the constraints were mobile enough for the hysteresis-free, highly reversible spectral changes to occur during the drying/soaking cycles or solvent switches. It hence indicates that nonpermanent, minor alterations in the conformation or packing (such as “bundling” as discussed above) may still proceed under the confinement within the brushes. Given this, the possibility of instigation by semi-permanent large-scale ordering, such as crystallization or “molecular aggregates” (which tend to give rise to red shifts, nevertheless), in the PL changes induced by the dry/soaking cycles can be reasonably ruled out.

For comparison, pristine MEH-PPV solid films emit light with a main peak at 570–590 nm (intrachain emissions), coupled with a secondary peak (or a shoulder) at ~ 590 nm (interchain emissions), and a minor component at ~ 640 nm owing to excimer emissions.^{16–18,25,50,51} For dilute solid solutions (single molecules embedded in inert solid matrix), λ_p is generally observed at ~ 550 nm.⁵² In contrast to the diminutive M dependence of solid films for $M > \sim 50$ kg/mol, the brush molecules illustrated a clear M dependence of λ_p in the M range explored here (up to 182 kg/mol; Figure 5e). The dependence, $\lambda_p \approx \beta M^2$, mimicked the electron-in-a-box model,¹¹ if the molar mass was scaled as the dimension (l) of the box with the energy levels defined as $E_n = (\hbar^2 / (2m^*))((n\pi)/l)^2$, where m^* is the effective electron mass and n is a positive integer. However, the large blue shifts relative to those of the solid films and solutions (e.g., $\Delta\lambda_p \sim 130$ nm for 55k MEH-PPV, Figure 3) implies the substantially shorter conjugation lengths for the brush molecules than hinted by the molar masses and thus indicates further investigation is necessary.

The large blue shifts of the brushes relative to free molecules, nevertheless, may be related to the steric hindrance operative during the graft-polymerization. Since the tether spacing ($d \sim 0.5$ nm) was significantly smaller than the side-group dimension of the monomer (~ 0.9 nm), a sizable portion of monomer misalignments in the growing chains was trapped, disrupting the π -conjugation and leading to short conjugation lengths. As the chains extended farther away from the substrate, the steric hindrance decreased progressively, as manifested precisely by the redder emissions of the longer brush molecules.

PL of the Pancakes. For tether spacings substantially greater than the MEH-PPV molecular dimensions, the PL spectra of the solvent-swollen samples were very similar to those of the free polymers of the same molar masses in the solutions (Figure 4b,c). This is consistent with the molecular attachment process believably operative in the graft-to reaction and is in good agreement with the fact that the graft density was found limited by the macromolecule size. In contrast to the brush molecules, the PL spectra exhibited a remarkable blue shift and an increase of PL intensity when dried in air. The spectral shift strongly depended on tether spacing d (Figure 4a). For example, for the $M = 55$ kg/mol polymer, λ_p shifted from 550 nm (in toluene) to 460 nm ($d = 10$ nm), 455 nm ($d = 14.5$ nm), 452 nm ($d = 20$ nm), or 434 nm ($d = 28$ nm). Similarly, for $M = 16$ kg/mol, λ_p moved from 470 nm (in toluene) to 434 nm ($d = 6$ nm), 420 nm ($d = 9$ nm), or 410 nm ($d = 15$ nm). The shifting and the intensity variation were fully reversible upon resubmergence (Figure 4b). Furthermore, the blue shift was dependent on the solvent evaporation rate in that it decreased when solvent evaporation was substantially slowed. For example, λ_p moved to 490 nm ($d = 10.5$ nm, $M = 55$ kg/mol, Figure S4, Supporting Information), rather than 460 nm for the quickly dried (Figure 4c). In addition to the λ_p shift, the PL spectra broadened upon drying, indicating a wider and more

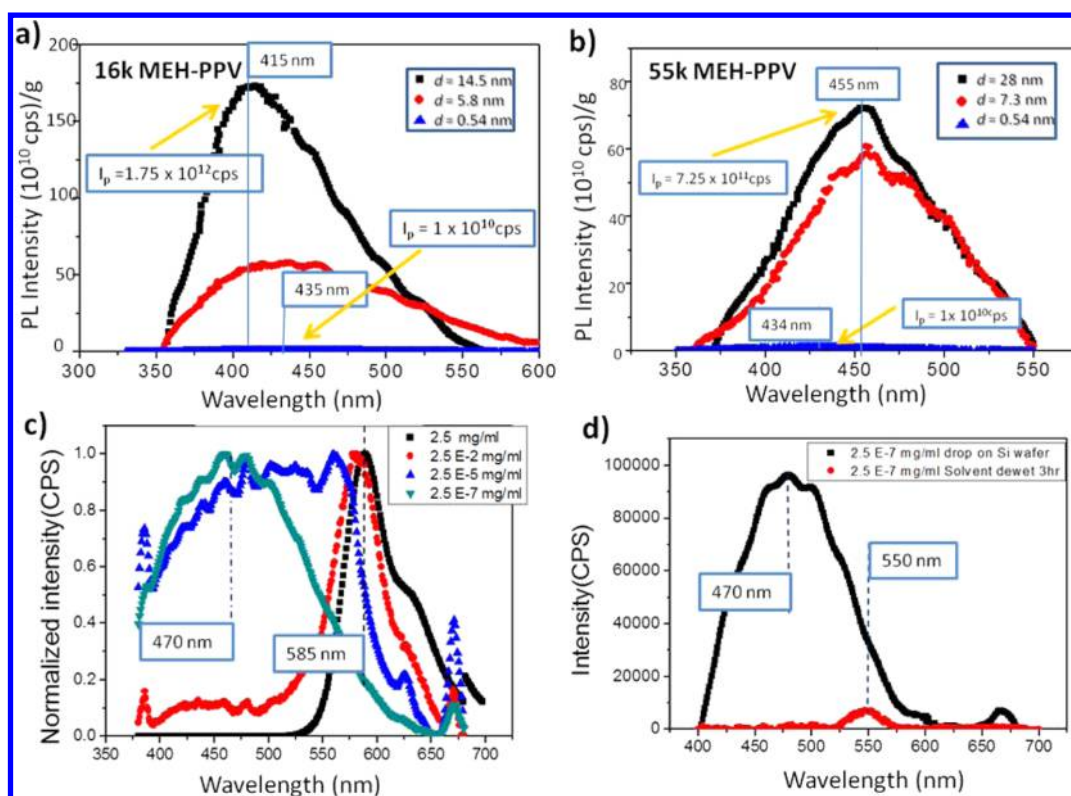


Figure 5. PL spectra of the MEH-PPV pancakes and drop-coated films. (a, b) Mass-normalized for the pancakes for various tether spacings d s annotated with the PL intensity I_p for $M = 16$ kg/mol (a) and $M = 55$ kg/mol, (b) the peak-normalized, please see Supporting Information, section 6. (c) Peak-normalized spectra of drop-coated MEH-PPV ($M = 55$ kg/mol) for various concentrations. (d) Mass-normalized spectra of drop-coated MEH-PPV from the very dilute solution ($c = 250$ ng/mL) before and after solvent annealing.

complicated distribution of the conjugation lengths in the dried pancake molecules.

The drying-induced spectra changes were attributed to the effects of mechanical stretching triggered by molecular contraction during the rapid solvent evaporation. The rapid molecular contraction under the influence of substrate anchoring gave rise to changes in molecular conformation as well as the rise of mechanical stress operative on the molecular strands, producing the blue shifts and the PL enhancements. The increase of PL intensity was in the order of 2–4-fold (Figure 4b,c) when compared with that in the solvent-swollen state. However, the PL behavior in the solvent-swollen state was strongly influenced by solvent plasticization so that exciton trapping may have been substantially reduced to obscure the comparison to that in the dry state. As will be detailed in the next section, the stress-induced PL enhancements were far more massive when dry samples were compared.

In order to study the process of PL measurement alterations during drying, an in situ PL experiment was undertaken where a wet sample was drying slowly between glass plates (right, Figure 1b) while being probed by a 473 nm laser in the confocal micro-PL spectrometer. It was found that the PL intensity decreased progressively as solvent evaporated (Figure 4d), indicating the decrease of the plasticization effect and the shift of photoexcitation threshold to beyond $\lambda = 473$ nm. This was despite the increase of both the excitation and detection efficiencies, arising from the drying-induced molecular alignment toward the substrate perpendicular to the beams. Moreover, during the drying no new PL peaks were arising and the main peak (at $\lambda_p = 550$ nm) was not shifting. Only when the pancakes were nearly dry, a new peak emerged,

replacing the diminishing main peak (Figure 4d). It suggests that the variation of the absorption and emission was of a discontinuous nature, mimicking a bistate discrete transition.

Effects of Segmental Stretching. The effect on PL intensity by mechanical stretching upon drying was further examined by comparing the dry samples (the pancakes and brushes) of different d s but of the same molar mass. It was found that, for $M = 16$ kg/mol, the PL intensity per MEH-PPV molecule increased approximately 175-fold as d increased from 0.5 to 14.5 nm (Figure 5a). For $M = 55$ kg/mol, it increased approximately 73-fold for d increasing from 0.5 to 28 nm (Figure 5b).

Clearly, these enormous PL enhancements were not due to any dipole realignment engendered by varying d , because the contribution of the latter was quite small, to be below ~ 1.5 -fold, calculated from $(1 + \sin^2 \theta) / \cos^2 \theta$ for the extreme case of dipoles alteration from perfect upright to totally lying down (see section 5, Supporting Information) where the beam incident angle θ was 45° (Horiba spectrometer, Experimental Section). Neither were due to the “molecular aggregation” because red shifts, instead of the blue shifts, would have been observed.^{7,18} Furthermore, similar to the brush MEH-PPV, the facile cycles of drying and re-soaking leading to the fully reversible PL shifting (Figure 4b,c) were sufficient to preclude any major role of semipermanent, intersegmental bondings in the drying of the pancake molecules.

Analogous to the mechanical forces induced in the solution casting of ultrathin polymer films that “squeeze” the giant molecules into dimensions smaller than the molecular sizes,^{22,23,53,54} substantial mechanical stresses were present in the MEH-PPV pancakes dried on the substrate on which the

rapid lateral retraction of the molecules gave rise to molecular kinks and the stretched chain segments. The π -conjugation was disrupted at these kinks resulting the blue shifts while the mechanical stretching of the molecular segments between them produced the enhanced PL emissions.^{16–18} The increase of the blue shift with tether spacing indicates that the molecular contraction was influenced by the neighboring chains even for the pancakes. Obviously, the smaller grafting density, the closer the molecule can get to a more unperturbed retraction, hence leading to shorter conjugation lengths and stronger PL emission enhancements in the dry state (Fig. 5a). Moreover, the dependence of the blue shift on solvent evaporation rate suggests the possibility of controlling the formation of these molecular kinks via manipulation of the drying-induced molecular movements.

The massive PL enhancements by drying unveiled yet another important effect of the mechanical stress. As discussed in the above that the Si-wafer was a strong exciton quencher for the MEH-PPV samples thinner than exciton diffusion length ~ 30 nm,^{11,18} the PL of the dry pancake molecules ($\tau < 2$ nm) would have been quenched much more substantially compared to that for the equivalent dry brushes ($\tau \sim 62$ nm for $M = 55$ kg/mol, Figure 2b). The fact that the dry pancakes emitted about 2 orders brighter than the brush molecules indicates that mechanical stretching had substantially decreased this quenching effect. This observation is in excellent agreement with the emission behavior of the stretched MEH-PPV molecules in the residual monolayer (~ 2 – 3 nm thick) produced by dewetting on the Si-wafer.¹⁸

Free Molecules under Mechanical Stresses. The drying-induced effects were also investigated for the untethered free molecules ($M = 55$ kg/mol) prepared by drop-coating on a Si-wafer. The PL spectra of the samples prepared from the concentrated solutions ($c > c^*$ or $c \sim c^* = 5 \times 10^{-2}$ mg/mL) were similar to that of pristine solid films ($\lambda_p \sim 585$ nm), red-shifting slightly relative to $\lambda_p \sim 560$ nm of the solvent-swollen polymer (Figure 3), consistent with the fact that the solvated molecules in the concentration solution were interpenetrating and dried as an entangled molecular network. Isolated MEH-PPV macromolecules were deposited on the Si-wafer when the concentration in the solution was reduced 5 orders of magnitude to substantially below c^* (i.e., $c = 250$ ng/mL). The spectrum was blue-shifted ~ 90 nm relative to the solutions to ~ 470 nm (Figure 5c). The peak position was comparable to those of the dried pancakes (~ 455 nm), indicating that the segmental stretching from the rapid solvent loss was similar to that in the dried pancakes. Finally, for samples prepared from the intermediate concentrations (2.5×10^{-7} mg/mL $< c < 2.5 \times 10^{-2}$ mg/mL), a broadened peak ranging from ~ 470 nm to ~ 585 nm was observed (Figure 5c), while the morphology under the confocal microscope and SFM revealed the coexistence of those corresponding to both the concentrated and the dilute solutions.

For the drop-coated, untethered isolated molecules from the highly diluted solutions, the mechanical stress may be removed by solvent annealing. After imbibing the sample in toluene vapor for 3 h, the PL spectrum red-shifted to $\lambda_p = 550$ nm (Figure 5d), returning to the emission wavelength reported for the single isolated MEH-PPV molecules embedded in PS matrix.⁵² Concomitantly, a decrease of PL intensity by a factor of 15 was observed. Obviously, these were caused by the release of the mechanical stresses exerting on the molecular segments,

in excellent agreement with the previous results of the tethered molecules.

Clearly, the brush molecules were confined by their neighbors anchored at merely one end-point on the substrate, and the constraints, although large enough to contain the solvent plasticization effect, were not sufficient to support strong stresses for suppressing the electron–phonon interactions, rendering them mechanically relaxed and highly susceptible to exciton trapping. Therefore, the MEH-PPV brushes were poor emitters in both the dry and solvent-swollen state. Conversely, the on-substrate retraction of the pancake molecules during drying provided opportunities of forming substrate anchoring spots for the molecular strands via local monomer pileup or chain entanglements, that may effectively introduce mechanical stresses to the molecular segments in the dried molecules to result in greatly enhanced PL efficiencies. Similar mechanisms were operative for the drop-coated isolated molecules. Finally, although both the PL intensity and the emission colors λ_p s were strongly influenced by mechanical stresses, the respective interaction mechanisms were discernible, as shown here by the conformation-specific CPs of pancakes, free molecules, and brushes. Alteration of PL colors comes along with efficiency enhancements only when the mechanical stretching has also altered the conjugation lengths. These observations are consistent with the behavior of stretched conjugated polymers observed in other systems.^{16–18}

Finally, given the observations presented in the above on the PL behavior of conformation-controlled MEH-PPV molecules in both the solutions and dry states, the dramatic effects on polymer photonics due to changes of the mechanical state have been clearly unveiled. The contributions possibly from other factors (e.g., substrate absorption, segmental anisotropy, molecular aggregation, and crystallization), as discussed in the preceding sections, were carefully examined and properly attributed. In this, the effect of substrate absorption of the light had been shown to be negligible (please see Supporting Information, section 3, for further information), and the influences of chain alignment (arising from changes induced during the dry/soaking transition) relative to the excitation and collection beam were analyzed and determined to be insignificant (please see Supporting Information, section 5, for further information). Furthermore, the reversibility of PL variations induced in the dry/soaking cycles clearly unveiled the insignificance of the effects arising from strong segmental aggregation or chain crystallization. Careful control over the molecular conformation and chain packing via designed polymer synthesis and well-managed soaking and drying processes had provided the opportunity for these important mechanical stress effects to be observed.

CONCLUSIONS

In conclusion, PL emission of conjugated polymers is highly dependent on the state of mechanical stresses operative in the molecular segments. As shown by the dry pancakes and drop-coated single molecules, mechanical stress may suppress exciton–phonon coupling, giving rise to significantly enhanced optoelectronic efficiencies. Mechanical stress may also reduce exciton quenching at a heterojunction where a large built-in electric field is operative. Clearly, mechanical stress plays a fundamental role in the optoelectronic behavior of conjugated polymers and hence should be taken into account in the design and manufacturing of the polymer-based optoelectronic devices.

■ ASSOCIATED CONTENT

■ Supporting Information

Additional information regarding (1) the reaction scheme of the MEH-PPV monomer, (2) the procedures of substrate priming, (3) effects of the silicon substrate on PL, (4) PL spectrum of the slow-drying brushes vs that via fast evaporation, (5) analysis of the molecular anisotropy effect on PL intensity measurements, and (6) PL spectra of MEH-PPV pancakes (peak-normalized). This material is available free of charge via the Internet at <http://pubs.acs.org>.

■ AUTHOR INFORMATION

Corresponding Author

*E-mail: acyang@mse.nthu.edu.tw.

Author Contributions

‡These authors contributed equally to this work (K.S.S. and C.C.C.).

Notes

The authors declare no competing financial interest.

■ ACKNOWLEDGMENTS

We greatly appreciate the advice and technical support kindly offered by Prof. Sue-Lein Wang of National Tsing Hua University, Taiwan, and the inspiring discussions with Prof. Günter Reiter of the University of Freiburg, Germany. We also thank the financial support by the National Science Council of Taiwan, and the U.S. Air Force Office of Scientific Research through the Taiwan–U.S. Air Force Nanoscience Initiative Program (AOARD-114055, -124064, and -134026).

■ REFERENCES

- (1) MacDiarmid, A. G.; Epstein, A. J. Polyanilines: a Novel Class of Conducting Polymers. *Faraday Discuss., Chem. Soc.* **1989**, *88*, 317–332.
- (2) Burroughes, J. H.; Bradley, D. D. C.; Brown, A. R.; Marks, R. N.; Mackay, K.; Friend, R. H.; Burns, P. L.; Holmes, A. B. Light-Emitting Diodes Based on Conjugated Polymers. *Nature* **1990**, *347*, 539–541.
- (3) Yang, Y.; Heeger, A. J. Polyaniline as a Transparent Electrode for Polymer Light-Emitting Diodes: Lower Operating Voltage and Higher Efficiency. *Appl. Phys. Lett.* **1994**, *64*, 1245–1247.
- (4) Krebs, F. C.; Spanggaard, H.; Kjær, T.; Biancardo, M.; Alstrup, J. Large Area Plastic Solar Cell Modules. *Mater. Sci. Eng., B* **2007**, *138*, 106–111.
- (5) Vanden Bout, D. A.; Yip, W.-T.; Hu, D.; Fu, D.-K.; Swager, T. M.; Barbara, P. F. Discrete Intensity Jumps and Intramolecular Electronic Energy Transfer in the Spectroscopy of Single Conjugated Polymer Molecules. *Science* **1997**, *277*, 1074–1077.
- (6) Lecuiller, R.; Berrehar, J.; Lapersonne-Meyer, C.; Schott, M. Dual Resonance Fluorescence of Polydiacetylene Chains Isolated in Their Crystalline Monomer Matrix. *Phys. Rev. Lett.* **1998**, *80*, 4068–4071.
- (7) Nguyen, T.-Q.; Martini, I. B.; Liu, J.; Schwartz, B. J. Controlling Interchain Interactions in Conjugated Polymers: The Effects of Chain Morphology on Exciton-Exciton Annihilation and Aggregation in MEH-PPV Films. *J. Phys. Chem. B* **2000**, *104*, 237–255.
- (8) Vogelsang, J.; Brazard, J.; Adachi, T.; Bolinger, J. C.; Barbara, P. F. Watching the Annealing Process One Polymer Chain at a Time. *Angew. Chem., Int. Ed.* **2011**, *50*, 2257–2261.
- (9) Onda, S.; Kobayashi, H.; Hatano, T.; Forumaki, S.; Habuchi, S.; Vacha, M. Complete Suppression of Blinking and Reduced Photo-bleaching in Single MEH-PPV Chains in Solution. *Phys. Chem. Lett.* **2011**, *2*, 2827–2831.
- (10) Guillet, T.; Berrehar, J.; Grousson, R.; Kovensky, J.; Lapersonne-Meyer, C.; Schott, M.; Voliotis, V. Emission of a Single Conjugated Polymer Chain Isolated in Its Single Crystal Monomer Matrix. *Phys. Rev. Lett.* **2001**, *87*, 087401–1–087401–4.

(11) Fox, M. *Optical Properties of Solids*; Oxford University Press: New York, 2001; Chapter 8.

(12) Mott, N. F. Conduction in Glasses Containing Transition Metal Ions. *J. Non-Cryst. Solids* **1968**, *1*, 1–17.

(13) Prins, P.; Grozema, F. C.; Schins, J. M.; Patil, S.; Scherf, U.; Siebbeles, L. D. A. High Intrachain Hole Mobility on Molecular Wires of Ladder-Type Poly(*p*-phenylenes). *Phys. Rev. Lett.* **2006**, *96*, 146601–1–146601–4.

(14) Bredas, J.-L.; Silbey, R. Excitons Surf along Conjugated Polymer Chains. *Science* **2009**, *323*, 348–349.

(15) Collini, E.; Scholes, G. D. Coherent Intrachain Energy Migration in a Conjugated Polymer at Room Temperature. *Science* **2009**, *323*, 369–373.

(16) Tung, K.-P.; Chen, C.-C.; Lee, P.; Liu, Y.-W.; Hong, T.-M.; Hwang, K. C.; Hsu, J. H.; White, J. D.; Yang, A. C.-M. Large Enhancements in Optoelectronic Efficiencies of Nano-Plastically Stressed Conjugated Polymer Strands. *ACS Nano* **2011**, *5*, 7296–7302.

(17) Lee, P.; Li, W. C.; Chien, Y.; Reiter, G.; Yang, A. C.-M. Photoluminescence Influenced by Chain Conformation in Thin Conjugated Polymer Films by Spin Coating and Dewetting, American Physical Society March Meeting, Dallas, TX, U.S.A., March 20–25, 2011, APS: College Park, MD, 2011.

(18) Lee, P.; Li, W.-C.; Chen, B.-J.; Yang, C.-W.; Chang, C.-C.; Botiz, I.; Reiter, G.; Lin, T. L.; Tang, J.; Yang, A. C.-M. Massive Enhancement of Photoluminescence through Nanofilm Dewetting. *ACS Nano* **2013**, *7*, 6658–6666.

(19) Sugimoto, T.; Habuchi, S.; Ogino, K.; Vacha, M. Conformation-Related Exciton Localization and Charge-Pair Formation in Polythiophenes: Ensemble and Single-Molecule Study. *J. Phys. Chem. B* **2009**, *113*, 12220–12226.

(20) Becker, K.; Lagoudakis, P. G.; Gaefke, G.; Hoger, S.; Lupton, J. M. Exciton Accumulation in *p*-Conjugated Wires Encapsulated by Light-Harvesting Macrocycles. *Angew. Chem., Int. Ed.* **2007**, *46*, 3450–3455.

(21) Thomsson, D.; Camacho, R.; Tian, Y.; Yadav, D.; Sforazzini, G.; Anderson, H. L.; Scheblykin, I. G. Cyclodextrin Insulation Prevents Static Quenching of Conjugated Polymer Fluorescence at the Single Molecule Level. *Small* **2013**, *9*, 2619–2627.

(22) Yang, M. H.; Hou, S. Y.; Chang, Y. L.; Yang, A. C.-M. Molecular Recoiling in Polymer Thin Film Dewetting. *Phys. Rev. Lett.* **2006**, *96*, 066105–1–066105–4.

(23) Al Akhrass, S.; Reiter, G.; Hou, S. Y.; Yang, M. H.; Chang, Y. L.; Chang, F. C.; Wang, C. F.; Yang, A. C.-M. Viscoelastic Thin Polymer Films under Transient Residual Stresses: Two-Stage Dewetting on Soft Substrates. *Phys. Rev. Lett.* **2008**, *100*, 178301–1–178301–4.

(24) Huang, L. C. Optical Harvesting Polymers in Carbon Nanotubes Network. *Master Thesis*, National Tsing Hua University, Taiwan, 2008.

(25) Padmanaban, G.; Ramakrishnan, S. Conjugation Length Control in Soluble Poly[2-methoxy-5-((2'-ethylhexyl)oxy)-1,4-phenylenevinylene] (MEHPPV): Synthesis, Optical Properties, and Energy Transfer. *J. Am. Chem. Soc.* **2000**, *122*, 2244–2251.

(26) Siqueira, D. F.; Kohler, K.; Stamm, M. Structures at the Surface of Dry Thin Films of Grafted Copolymers. *Langmuir* **1995**, *11*, 3092–3096.

(27) Becker, H.; Spreitzer, H.; Kreuder, W.; Kluge, E.; Schenk, H.; Parker, I.; Cao, Y. Soluble PPVs with Enhanced Performance: A Mechanistic Approach. *Adv. Mater.* **2000**, *12*, 42–48.

(28) Becker, H.; Spreitzer, H.; Ibrom, K.; Kreuder, W. New Insights into the Microstructure of GILCH-Polymerized PPVs. *Macromolecules* **1999**, *32*, 4925–4932.

(29) Williams, K. R.; Muller, R. S. Etch Rates for Micromachining Processing. *J. Microelectromech. Syst.* **1996**, *5*, 256–269.

(30) Williams, K. R.; Gupta, K.; Wasilik, M. Etch Rates for Micromachining Processing: Part II. *J. Microelectromech. Syst.* **2003**, *12*, 761–778.

- (31) Graf, D.; Grundner, N.; Schulz, R. Reaction of Water with Hydrofluoric Acid Treated Silicon (111) and (100) Surfaces. *J. Vac. Sci. Technol. A* **1989**, *7*, 808–813.
- (32) Khanduyeva, N.; Senkovskyy, V.; Beryozkina, T.; Horecha, M.; Stamm, M.; Uhrich, C.; Riede, M.; Leo, K.; Kiriy, A. Surface Engineering Using Kumada Catalyst-Transfer Polycondensation (KCTP): Preparation and Structuring of Poly(3-hexylthiophene)-Based Graft Copolymer Brushes. *J. Am. Chem. Soc.* **2009**, *131*, 153–161.
- (33) Van Der Voort, P. F.; Vansant, E. F. Silylation of the Silica Surface: A Review. *J. Liq. Chromatogr. Relat. Technol.* **1996**, *19*, 2723–2752.
- (34) Okabayashi, H.; Shimizu, I.; Nishio, E.; O'Connor, C. J. Diffuse Reflectance Infrared Fourier Transform Spectral Study of the Interaction of 3-Aminopropyltriethoxysilane on Silica Gel. Behavior of Amino Groups on the Surface. *Colloid Polym. Sci.* **1997**, *275*, 744–753.
- (35) Takahagi, T.; Ishitani, A.; Kuroda, H.; Nagasawa, Y. Fluorine-Containing Species on the Hydrofluoric Acid Etched Silicon Single-Crystal Surface. *J. Appl. Phys.* **1991**, *69*, 803–807.
- (36) Wirth, M. J.; Fatunmbi, H. O. In *Chemically Modified Surface*; Pesek, J. J., Leigh, I. E., Eds.; Royal Society of Chemistry: London, 1994; p 253.
- (37) Krasnoslobodtsev, A. V.; Smirnov, S. N. Effect of Water on Silanization of Silica by Trimethoxysilanes. *Langmuir* **2002**, *18*, 3181–3184.
- (38) Zhang, F.; Srinivasan, M. P. Self-Assembled Molecular Films of Aminosilanes and Their Immobilization Capacities. *Langmuir* **2004**, *20*, 2309–2314.
- (39) Plueddemann, E. P. *Silane Coupling Agents*; Plenum: New York, 1991.
- (40) Trens, P.; Denoyel, R.; Rouquerol, J. Adsorption of (γ -Aminopropyl) triethoxysilane on Silica from Aqueous Solution: A Microcalorimetric Study. *Langmuir* **1995**, *11*, 551–554.
- (41) Chiang, C.-H.; Liu, N.-I.; Koenig, J. L. Magic-Angle Cross-Polarization Carbon 13 NMR Study of Aminosilane Coupling Agents on Silica Surfaces. *J. Colloid Interface Sci.* **1982**, *86*, 26–33.
- (42) Zhuravlev, L. T. Concentration of Hydroxyl Groups on the Surface of Amorphous Silicas. *Langmuir* **1987**, *3*, 316–318.
- (43) Heiney, P. A.; Gruneberg, K.; Fang, J.; Dulcey, C.; Shashidhar, R. Structure and Growth of Chromophore-Functionalized (3-Aminopropyl)triethoxysilane Self-Assembled on Silicon. *Langmuir* **2000**, *16*, 2651–2657.
- (44) Milner, S. T. Polymer Brushes. *Science* **1991**, *251*, 905–914.
- (45) Sontag, S. K.; Marshall, N.; Locklin, J. Formation of Conjugated Polymer Brushes by Surface-Initiated Catalyst-Transfer Polycondensation. *Chem. Commun.* **2009**, *23*, 3354–3356.
- (46) Beinhoff, M.; Appapillai, A. T.; Underwood, L. D.; Frommer, J. E.; Carter, K. R. Patterned Polyfluorene Surfaces by Functionalization of Nanoimprinted Polymeric Features. *Langmuir* **2006**, *22*, 2411–2414.
- (47) Luzinov, I.; Julthongpipit, D.; Malz, H.; Pionteck, J.; Tsukruk, V. V. Polystyrene Layers Grafted to Epoxy-Modified Silicon Surfaces. *Macromolecules* **2000**, *33*, 1043–1048.
- (48) Koutsos, V.; van der Vegte, E. W.; Pelletier, E.; Stamouli, A.; Hadziioannou, G. Structure of Chemically End-Grafted Polymer Chains Studied by Scanning Force Microscopy in Bad-Solvent Conditions. *Macromolecules* **1997**, *30*, 4719–4726.
- (49) Atreya, M.; Li, S.; Kang, E. T. Stability Studies of Poly(2-methoxy-5-(20-ethyl hexyloxy)-*p*-(Phenylene vinylene) [MEH-PPV]. *Polym. Degrad. Stab.* **1999**, *65*, 287–296.
- (50) Collison, C. J.; Rothberg, L. J.; Treemanekarn, V.; Li, Y. Conformational Effects on the Photophysics of Conjugated Polymers: A Two Species Model for MEH-PPV Spectroscopy and Dynamics. *Macromolecules* **2001**, *34*, 2346–2352.
- (51) Cossello, R. F.; Kowalski, E.; Rodrigues, P. C.; Akcelrud, L.; Bloise, A. C.; deAzevedo, E. R.; Bonagamba, T. J.; Atvars, T. D. Z. Photoluminescence and Relaxation Processes in MEH-PPV. *Macromolecules* **2005**, *38*, 925–932.
- (52) Barbara, P. F.; Gesquiere, A. J.; Park, S.-J.; Lee, Y. J. Single Molecule Spectroscopy of Conjugated Polymers. *Acc. Chem. Res.* **2005**, *38*, 602–610.
- (53) Reiter, G.; Hamieh, M.; P. Damman, P.; Scavons, S.; Gabriele, S.; Vilmin, T.; Raphael, E. *Nat. Mater.* **2005**, *4*, 754.
- (54) Chang, Y. L. Measurements and Analysis of the Molecular Stresses, Packing, and Deformations of Polymer Coils Confined in Spin-Coated Thin Films. *Master Thesis*, National Tsing Hua University, Taiwan, 2008.